

Instant Visual Detection of Picogram Levels of Trinitrotoluene by Using Luminescent Metal–Organic Framework Gel-Coated Filter Paper

Ji Ha Lee,^[a] Sunwoo Kang,^[b] Jin Yong Lee,^{*,[b]} Justyn Jaworski,^[c] and Jong Hwa Jung^{*,[a]}

Abstract: There is an ongoing need for explosive detection strategies to uncover threats to human security including illegal transport and terrorist activities. The widespread military use of the explosive trinitrotoluene (TNT) for landmines poses another particular threat to human health in the form of contamination of the surrounding environment and groundwater. The detection of explosives, particularly at low picogram levels, by using a molecular sensor is seen as an important chal-

lenge. Herein, we report on the use of a fluorescent metal–organic framework hydrogel that exhibits a higher detection capability for TNT in the gel state compared with that in the solution state. A portable sensor prepared from filter paper coated by the hydrogel was able to detect TNT at the picogram

level with a detection limit of 1.82 ppt (parts per trillion). Our results present a simple and new means to provide selective detection of TNT on a surface or in aqueous solution, as afforded by the unique molecular packing through the metal–organic framework structure in the gel formation and the associated photophysical properties. Furthermore, the rheological properties of the MOF-based gel were similar to those of a typical hydrogel.

Keywords: explosives • gels • metal–organic frameworks • sensors • supramolecular chemistry

Introduction

Trinitrotoluene (TNT) is an explosive chemical, in wide use by militaries, existing in a variety of formulations and degradation products that are harmful to human health and the environment.^[1–5] As a result, the selective detection of TNT has been a matter of great concern to scientists.^[6] Although a number of reports exist on the topic of explosive detection, a simple approach to the detection of TNT at extremely low concentrations still remains a challenge.^[7–11] Due to the relatively low vapor pressure of TNT, particularly in comparison to other explosive chemicals, the detection of low quantities of TNT is particularly challenging.^[12] The groups of Swager^[13–19] and Trogler^[20–24] have made significant advances in the detection of TNT. Swager et al. reported improved fluorescence quenching associated with the nitroaromatic binding events in aggregated systems and solid films

of conjugated polymers as a result of intermolecular exciton migration and also through multi-photon fluorescence quenching, thereby providing a means for ultrasensitive detection of TNT. Consequently, several approaches using quantum dots,^[9,25] gold nanoparticles,^[26,27] and molecular imprinting with AuNPs^[28,29] have been reported for the detection of TNT. Recently, Zang et al.^[30] have also reported on the selective detection of TNT by implementing nanoporous nanofibers fabricated from carbazole-based tetracycles that are strongly encapsulated in the nanopores.

Compared with individual aromatic molecules, the self-assembly of nano-architectures from these building-block components can have strikingly different properties.^[31–35] The property of fluorescence response, for example, can often show significant changes depending on the surrounding medium. In some cases, molecules can even fluoresce as a consequence of gelation and have shown remarkable modulations of the emission color and intensity, which are reversible with external stimuli.^[36,37] Self-assembled gels with such fluorescence properties are, therefore, useful candidates for the detection of various analytes, including explosive compounds, cationic species, and anionic species.^[38–43] In particular, Berke et al.^[44] has reported the selective detection of nitroaromatic compounds by using an Al-based metal–organic framework gel. Whereas such organic conjugated polymers and nanomaterials have shown successful detection of explosive compounds with high sensitivity, the visual detection of explosives at the picogram level by using metal–organic framework gels remains a valuable goal and a challenge worth undertaking. With this in mind, we herein report the formation of a metal–organic framework hydro-

[a] J. H. Lee, Prof. Dr. J. H. Jung
Department of Chemistry and
Research Institute of Natural Sciences
Gyeongsang National University, Jinju 660-701 (Korea)
Fax: (+82)55-772-1488
E-mail: jonghwa@gnu.ac.kr

[b] S. Kang, Prof. Dr. J. Y. Lee
Department of Chemistry and Institute of Basic Science
Sungkyunkwan University, Suwon 440-746 (Korea)
E-mail: jinylee@skks.edu

[c] Prof. Dr. J. Jaworski
Department of Chemical Engineering
Hanyang University, Seoul 133-791 (Korea)

Supporting information for this article is available on the WWW under <http://dx.doi.org/10.1002/chem.201301507>.

gel in the presence of Zn^{2+} and its application as a chemosensor for the detection of low levels of TNT molecules.

Results and Discussion

In a solution of ethanol, compound **1** with Zn^{2+} was non-fluorescent, but upon gelation it emitted blue fluorescence (445 nm; Figure 1a and 1b). When gel **1-Zn**²⁺ was coated

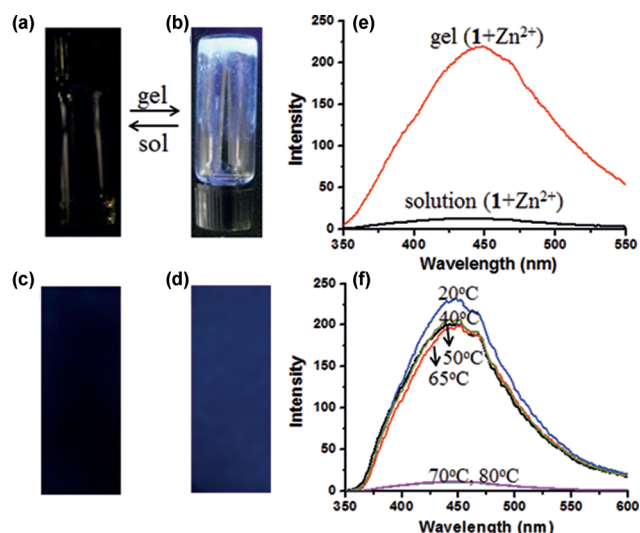
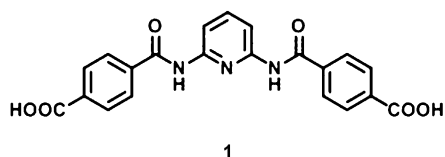


Figure 1. Photographs of (a) sol **1** (2.0 wt%) with Zn^{2+} (2.0 equiv) and (b) hydrogel **1** (2.0 wt%) with Zn^{2+} (2.0 equiv); (c) Photographs of sol **1** with Zn^{2+} in ethanol and (d) hydrogel **1-Zn**²⁺-coated filter papers; (e) Fluorescence spectra of hydrogel **1-Zn**²⁺ and sol **1** with Zn^{2+} in ethanol ($\lambda_{\text{ex}} = 302 \text{ nm}$); (f) Fluorescence spectra of hydrogel **1-Zn**²⁺ at different temperatures.

on filter paper, the blue emission persisted (Figure 1d). On the other hand, sol **1** (2.0 wt%) with Zn^{2+} -coated (2.0 equiv) filter paper showed non-emission (Figure 1c). In addition, the gel **1-Zn**²⁺ exhibited a strong emission, whereas the sol **1** with Zn^{2+} exhibited non-emission at the same concentration (Figure 1e). Fluorescence of the coordination polymer gel **1** also varied as a function of temperature (Figure 1f). The fluorescence intensity of gel **1-Zn**²⁺ slightly decreased at 65°C. Further increases in temperature resulted in a large decrease in emission. These results suggest that the emission of gel **1-Zn**²⁺ decreases as it starts to melt at 65–70°C. The optimal emission of **1-Zn**²⁺ therefore occurs when the gel is completely formed and decreases as the gel melts at higher temperature.



Scanning electron microscopy (SEM) images of gel **1-Zn**²⁺ when it was coated onto filter paper are shown in Figure S1 (the Supporting Information). The SEM image of gel **1-Zn**²⁺ revealed a typical fiber structure with diameter of 45–200 nm (Figure S1a, the Supporting Information). When the gel was applied to the filter paper, the paper was completely covered by the entangled gel fibers (45–200 nm) of the **1-Zn**²⁺ molecules (Figure S1b, the Supporting Information), which had a similar appearance to the gel **1-Zn**²⁺ itself. This finding supports the view that gel **1-Zn**²⁺ adheres well to the filter paper.

We prepared several samples of sol **1-Zn**²⁺ in ethanol to study the response of their fluorescence with different nitroaromatic compounds such as dinitrotoluene (DNT), *o*-nitrotoluene (ONT), nitromethane (NM), nitrobenzoic acid (NBA), methyl benzoate (MB), and isophthalate (IP; Figure S2, the Supporting Information). Our first attempt studied the fluorescence changes of **1** in the presence of Zn^{2+} in ethanol. The fluorescence intensity of **1** with Zn^{2+} ($1 \times 10^{-3} \text{ M}$) in a solution of ethanol was about 15-fold less than that of gel **1-Zn**²⁺, due to fast rotation of the phenyl rings. The fluorescence response of sol **1** (2.0 wt%) with Zn^{2+} (2.0 equiv) in ethanol upon addition of TNT (2.0–10.0 mM; Figure 2A) displayed a weak quenching of the fluorescence.

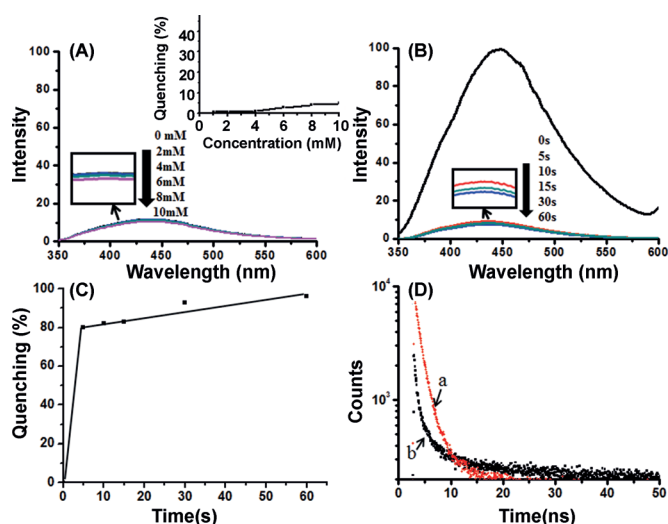


Figure 2. (A) Emission spectra of sol **1-Zn**²⁺ upon addition of TNT ($\lambda_{\text{ex}} = 302 \text{ nm}$). Inset: Plot of quenching (%) at 445 nm versus concentration of TNT; (B) Fluorescence spectra of gel **1-Zn**²⁺-coated filter paper upon addition of TNT ($1.0 \times 10^{-3} \text{ M}$); (C) Plot of fluorescence quenching (%) at 445 nm versus time in seconds; (D) Lifetime decay profiles of gel **1-Zn**²⁺ (a) before and (b) after addition of TNT ($1.0 \times 10^{-3} \text{ M}$) at room temperature.

These observations indicated that TNT is not an efficient quencher for **1** in the isotropic solution state and hence, this setup of a non-gelled solution of **1** is not suitable for the detection of TNT, but instead it requires the gel state. In addition, no significant quenching effects of the fluorescence of sol **1** with Zn^{2+} were obtained by exposure to DNT, ONT, NM, and NBA (Figure S2, the Supporting Information).

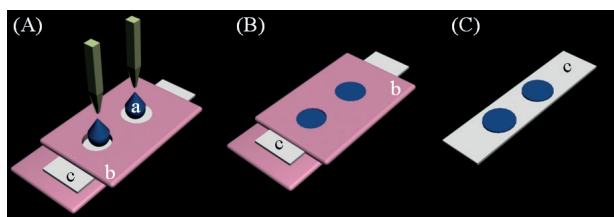


Figure 3. Images of the filter paper sensor (A) and (B) after addition of the hydrogel 1-Zn^{2+} ((a) gel 1-Zn^{2+} ; (b) plastic mask, and (c) filter paper); (C) Final sensor view.

For immobilized gel-based experiments, we cut the gel 1-Zn^{2+} -coated filter paper into strips of 2×5 cm and partially covered them with plastic masks of 3×6 cm on both sides (Figure 3). Details of these portable sensor components and assembly are schematically shown in Figure 3. When glued together, the two plastic masks on either side of the filter paper prevent any direct contact of gel 1-Zn^{2+} fibers with impurities. The small orifice (0.5 cm diameter) in the front mask allows room for casting the membrane. Then, a measured amount of hydrogel 1-Zn^{2+} (100 μL , 2.0 wt %) was dropped at the orifices on filter paper (0.5 cm diameter) and dried under vacuum (Figure 3). These filter papers were used as conventional chemosensors for TNT. The hydrogel 1-Zn^{2+} -coated filter paper was placed in a vial containing TNT at room temperature. The emission spectra were measured by using a front-face technique after exposing the film for specific intervals (Figure 2B). Surprisingly, significant quenching of the fluorescence was observed (Figure 2B and 2C) upon exposure to TNT solution. Nearly (90 ± 5)% quenching was noticed within 30 s of exposure (Figure 2C), indicating a fast response time and a detection limit of less than the ppb concentration level. To understand the excited-state behavior of the gel 1-Zn^{2+} , the fluorescence lifetime decay profiles before and after exposure to TNT were recorded. These data of hydrogel 1-Zn^{2+} ($\lambda_{\text{ex}} = 303$ nm) exhibited a biexponential character with lifetimes of 5.30 and 120.68 ns when monitored at 440 nm (Figure 2D; a). Upon exposure to TNT vapor, a fast biexponential decay with time constants of 3.95 and 62.16 ns was observed (Figure 2D; b). The decrease in the average lifetime can be attributed to the charge-transfer interaction of TNT with the self-assembled gel fibrils (specifically between the aromatic ring of TNT, which is electron-deficient, and the aromatic group of the **1** in the metal-organic framework, which is electron-rich).

In confocal laser scanning microscopy (CLSM) images of the hydrogel 1-Zn^{2+} before addition of a solution of TNT (Figure 4), the nanofiber of gel 1-Zn^{2+} showed a strong blue emission. At 10 s after the addition of TNT (10 ppm), the fluorescence emission of the nanofibers of hydrogel 1-Zn^{2+} was slightly quenched (Figure 4b), and upon addition of higher levels of TNT (100 ppm), almost complete quenching was observed (Figure 4c). These findings indicate that the fluorescence of gel 1-Zn^{2+} was more responsive in the gel phase as compared to the solution state. In addition, a single

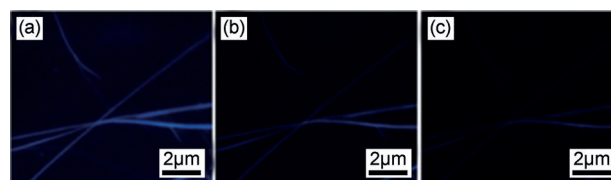


Figure 4. Confocal laser scanning microscopy (CLSM) images of hydrogel 1-Zn^{2+} upon addition of TNT (a) 0, (b) 10, and (c) 100 ppm.

nanofiber of gel 1-Zn^{2+} could sensitively detect TNT molecules.

During the preparation and packaging of explosive devices or during an explosion, particles of the explosive compound can contaminate the human body, clothing, and other materials in the surroundings. In such cases, it is desirable to check for residual contamination by an explosive chemical by using a contact-mode methodology. For this purpose, we transferred 1-Zn^{2+} gel fibers onto a Whatman filter paper by applying a hot solution of the gel to the paper (Figure S3, the Supporting Information), followed by drying under vacuum. The dried filter papers were then cut into strips. We considered that a contact-mode test for TNT contamination could be performed by extracting the target material with a suitable solvent, then dilution of the extract to the appropriate volume, and spot testing by application of the extract to the paper test strips.

We prepared acetonitrile solutions of different analytes (acetonitrile) and 100 μL of each solution was placed on the filter paper test strips coated by gel 1-Zn^{2+} to give a spot area of around 0.18 cm^2 . The visual fluorescence response of TNT at different concentrations by contact-mode detection on Whatman filter paper test strips is shown in Figure 5A. The minimum amount of TNT detectable by the naked eye was as low as 5.0 μL of a 1.0×10^{-12} M solution, thereby recording a detection limit of 1.82 parts per trillion (ppt). The fluorescence spectral changes of the test strips on contact with TNT for a wide range of concentration is shown in Figure 5B, and the corresponding fluorescence quenching (%) at 460 nm is shown in Figure 5C. A comparison of the minimum detectable amounts of the analytes estimated from the fluorescence quenching indicates that nonaromatic explosives and aromatic compounds without nitro groups are not sensed by the test strips (Figure 5D). Fluorescence quenching could be visually detected with these test strips to the level of 1.82×10^{-12} g (nitrotoluene; TNT), 2.27×10^{-10} g (dinitrotoluene; DNT), 1.37×10^{-10} g (*o*-nitrotoluene; ONT), 1.67×10^{-8} g (nitrobenzoic acid; NBA), 1.66×10^{-8} g (nitromethane; NM), and 1.67×10^{-4} g (toluene; T) when 100 μL of the analyte was spotted with a spread of about 0.18 cm^2 . From these data, the detection limit of TNT is calculated as around 1.82 pg cm^{-2} . Thus, the sensitivity of gel **1** with Zn^{2+} for TNT was as much as ≈ 100 times higher than that of DNT. Furthermore, in ambient light, the white color of the gel 1-Zn^{2+} was changed into a red color when TNT solution was added to the filter paper coated with the gel 1-Zn^{2+} (Figure S4, the Supporting Information), indicating that the

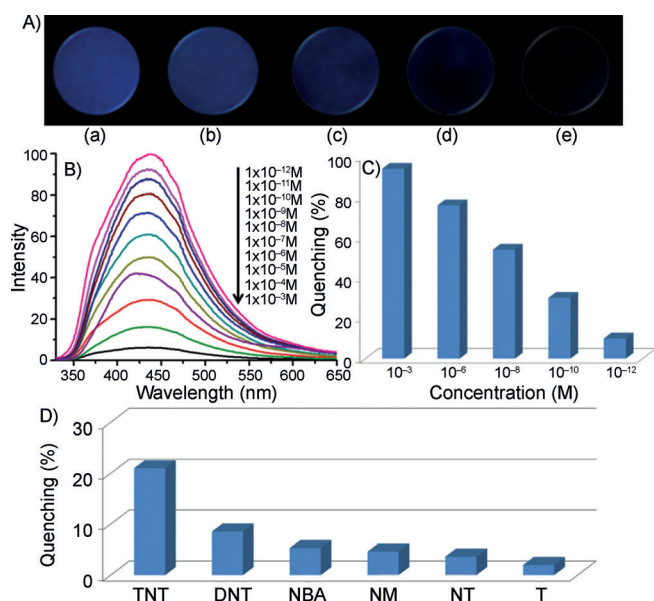


Figure 5. (A) Photographs of the fluorescence quenching of gel **1-Zn²⁺**-coated test strips by different concentration of TNT; (a) 0 M, (b) 1.0×10^{-12} M, (c) 1.0×10^{-10} M, (d) 1.0×10^{-8} M, and (e) 1.0×10^{-6} M; (B) Fluorescence spectral changes of the test strips on contact with added amount of TNT ($\lambda_{\text{ex}} = 302$ nm); (C) Plot of the quenching (%) against concentration of added TNT in acetonitrile; (D) Contact-mode detection of the lowest amount of different analytes (1.0×10^{-12} M) by the emission quenching test strip.

gel **1-Zn²⁺** acted as both a chromogenic and fluorogenic chemosensor for TNT. We have provided a comparison of our gel **1-Zn²⁺**-based detection system to several other approaches for TNT detection (Table 1), showing the merit of our system in terms of improved sensitivity.^[47–55]

To better understand, from a structural perspective, the molecular recognition process between **1-Zn²⁺** complex and TNT, we have carried out density functional theory (DFT) calculations using B3LYP hybrid functional with 6-31G* basis set implemented in Gaussian 09 programs (Figures 5 and S5 in the Supporting Information).^[45] In our calculations, we reduced the size of the host molecule containing two Zn²⁺ cations and six ligands due to the computational capability. The optimized structures of **1-Zn²⁺** as a host, **1-Zn²⁺·TNT**, appears in Figure 6. Similar to our previous report,^[46] each Zn²⁺ species was tetrahedrally coordinated by the oxygen atoms of the ligands. The inter-atomic distance between the two Zn²⁺ cations ($R_{\text{Zn} \cdots \text{Zn}}$) was calculated to be 18.82 Å and that between the two nitrogen atoms at the pyridine moieties ($R_{\text{N} \cdots \text{N}}$) was 11.72 Å in the host molecule. Moreover, the distances of $R_{\text{O} \cdots \text{O}}$ (oxygen atom at carboxyl group of ligand) were measured in the range of 3.050–3.426 Å. In binding with TNT, the value of $R_{\text{Zn} \cdots \text{Zn}}$ was calculated to be 18.18 Å for **1-Zn²⁺·TNT**, and the $R_{\text{N} \cdots \text{N}}$ was calculated to be 12.46 Å. Additionally, the $R_{\text{O} \cdots \text{O}}$ values for **1-Zn²⁺** with TNT were determined in the range of 3.152–3.435 Å. These results indicate that TNT induces a remarkable structural change of the host molecule. Whereas hydrogen bonding (HB) may play an important role with respect

Table 1. Comparison of sensors for the detection of TNT in aqueous solution.

Approach	LOD ^[a] [ppb]	Ref.
Imprinted electropolymerized oligoaniline-cross-linked AuNPs	0.046	[28]
Anti-2,4,6-trinitrophenol antibody surface plasmon resonance (SPR) immunoassay	0.09	[47]
Electrochemical sensor using mesoporous SiO ₂ of MCM-41 as modified electrode material	≈0.4	[48]
Adsorptive stripping voltammetric detection using a carbon nanotube-modified glassy carbon electrode	0.6	[49]
Commercially available colorimetric kits for TNT detection	1	[50]
Adsorptive stripping voltammetry using a nanocomposite-modified glassy carbon electrode (GC) containing Cu nanoparticles and SWCNT ^[b] solubilized in Nafion	1	[51]
Electrochemical detection by MWCNT ^[c] -functionalized electrodes	≈5	[52]
Competitive immunoassay for TNT detection as detected by QCM and SPR	1–10	[53]
Fiber-optic biosensor employing fluorescent evanescent wave-sensing with antibodies used as the recognition molecule	10	[54]
Luminescence from colloidal oligo(tetraphenyl)silole nanoparticle-based sensors	20	[22]
Electrochemical sensor using multiple carbon fibers as a working electrode	≈30	[55]

[a] LOD = limit of detection. [b] SWCNT = single-wall carbon nanotubes. [c] MWCNT = multi-walled carbon nanotubes.

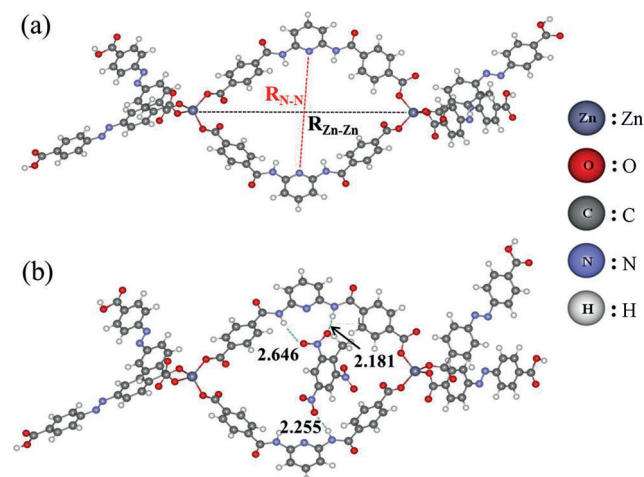


Figure 6. The optimized structure of a model system of gel **1-Zn²⁺** (a) before and (b) after addition of TNT.

to TNT in the cavity of the host, the calculated structure does not appear to account for the charge-transfer interactions observed. The detailed structural feature of HBs in two recognition systems indicated that three HBs exist in **1-Zn²⁺·TNT** with $\text{NH} \cdots \text{O}$ distances of 2.255, 2.181, and 2.646 Å. As expected, the calculated interaction energy be-

tween $\mathbf{1}\text{-Zn}^{2+}$ and TNT was calculated to be $7.32\text{ kcal mol}^{-1}$. The HBs existing in $\mathbf{1}\text{-Zn}^{2+}\cdot\text{TNT}$ can be characterized as typical HBs considering HB distances and interaction energies. It is important to note that other more preferred configurations may be revealed in more accurate models for London dispersion interaction. For example, one might have expected other configurations allowing charge-transfer interactions, such as $\pi\text{-}\pi$ stacking, to be in the predicted lowest-energy geometry. In addition, the small energy differences between host and guest (DNT and TNT) molecules can represent the selectivity of an appropriate guest molecule. We have only considered orbital energy levels of isolated DNT and TNT molecules, respectively, because the HOMO energy level of the isolated host is same. Thus, we have compared the LUMO energy levels of DNT and TNT. The calculated LUMO energy levels for DNT and TNT are -3.17 and -3.70 eV , indicating that the LUMO energy level of TNT is closer in energy than that of DNT to the HOMO energy level of the host.

The XRD patterns of gel $\mathbf{1}$ with Zn^{2+} before and after exposure to TNT are shown in Figure 7. The main reflection peaks appeared at 13.5 , 22.0 , 25.2 , 29.2 , and 39.5θ for 6.55 ,

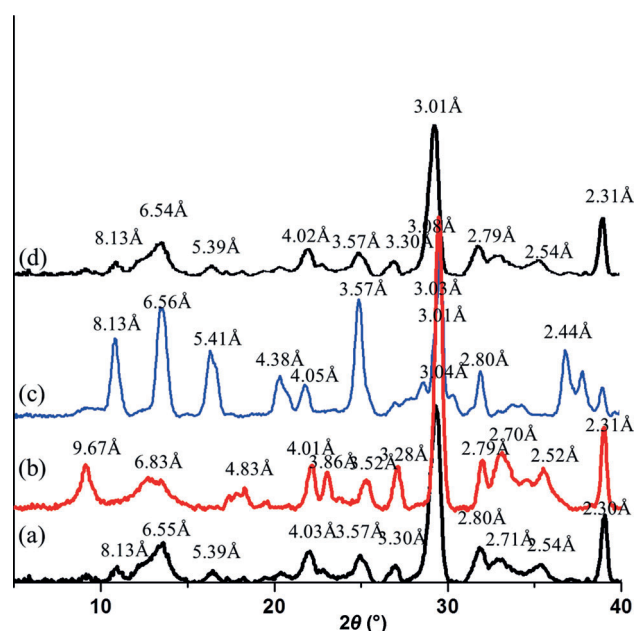


Figure 7. Powder XRD patterns of gel $\mathbf{1}\text{-Zn}^{2+}$ (a) before and after exposure to (b) TNT (3.0 equiv), (c) DNT (3.0 equiv), or (d) gel $\mathbf{1}\text{-Zn}^{2+}$ in acetonitrile.

4.03 , 3.57 , 3.03 , and 2.03 Å , respectively. The d -spacing of 8.13 Å corresponds to the distance between the alternate (top and bottom) ligand $\mathbf{1}$. Interestingly, gel $\mathbf{1}\text{-Zn}^{2+}$ -coated filter paper after exposure to saturated TNT vapors exhibited a large change in the XRD pattern. The reflection peaks were shifted to the small angle range. The largest d -spacing of 9.67 Å corresponds to the distance between the alternate (top and bottom) ligand. In particular, the new reflection

peak appeared at 23.2θ ; this peak, corresponding to a d -spacing of 3.86 Å , could be the π -stacking distance between the ligand molecule and the TNT molecule. On the other hand, after exposure to DNT vapors, only negligible changes were observed in the diffraction peaks, indicating that the packing of gel $\mathbf{1}$ is not considerably disturbed by DNT vapors. In addition, we measured the powder-XRD patterns of gel $\mathbf{1}\text{-Zn}^{2+}$ upon addition of methyl benzoate (MB), or isophthalate (IP; Figure S6, the Supporting Information). The powder XRD patterns of gel $\mathbf{1}\text{-Zn}^{2+}$ upon addition of methyl benzoate, or isophthalate were almost the same as that of gel $\mathbf{1}\text{-Zn}^{2+}$ itself. These results indicate that the TNT molecules are trapped inside the interstitial space of the ligand $\mathbf{1}\text{-Zn}^{2+}$ complexes, inducing changes in the overall molecular packing, and the observed fluorescence quenching is due to excited-state processes.

Rheological information is an indicator of the behavior of the gels when they are exposed to mechanical stress. The “storage” (or “elastic”) modulus G' represents the ability of the deformed material to “snap back” to its original geometry, and the “loss” (or “viscous”) modulus G'' represents the tendency of a material to flow under stress. Two rheological criteria required for a gel are: 1) the independence of the dynamic elastic modulus, G' , with respect to the oscillatory frequency, and 2) G' must exceed the loss modulus G'' by about one order of magnitude. We first used dynamic strain sweep to determine the proper conditions for the dynamic frequency sweep of the gels $\mathbf{1}\text{-Zn}^{2+}$. As shown in Figure S7A (the Supporting Information), the values of the storage modulus (G') and the loss modulus (G'') exhibited a weak dependence from 0.1 to 1.0% of strain (with G' dominating G''), indicating that the sample is a gel. The value of G' and of the gel $\mathbf{1}\text{-Zn}^{2+}$ were about 10-fold higher than that of G'' . We also used the dynamic frequency sweep to study the gel after setting the strain amplitude at 0.1% (within the linear response region of the strain amplitude). The values of G' and G'' were almost constant with the increase of frequency from 0.1 to 100 rad s^{-1} (Figure S7B, the Supporting Information). The value of G' was about 5 times larger than that of G'' over the whole range ($0.1\text{--}100\text{ rad s}^{-1}$), suggesting that the gel is fairly tolerant to external force. Furthermore, time-dependent oscillation measurements were used to monitor the gelation processes of gels $\mathbf{1}\text{-Zn}^{2+}$ (Figure S7C, the Supporting Information). The time sweep shows the rapid increase of G' and G'' in the initial stage of gelation, followed by a slower long-term approach to a final pseudo-equilibrium plateau. At the end of the experiment, the value of G' was about an order of magnitude higher than G'' .

Conclusion

Pictogram-level detection of TNT by using a fluorescent metal-organic framework nanomaterial has been demonstrated. The ligand $\mathbf{1}$ in the presence of Zn^{2+} in the solution state is not efficient for detecting TNT, whereas in the

metal–organic framework-based xerogel state we have achieved high sensitivity detection of TNT. These findings highlight the unique capability of the self-assembled fibrous structures as new materials with specific sensing applications. The detection level of metal–organic framework hydrogel **1** was in the ppt range in the contact mode. Pico-gram-level detection with high sensitivity, achieved by using portable filter paper-based test strips, allows a simple and low-cost protocol for the on-site instant detection of TNT on contaminated specimens. Such a strategy may be extended to other fluorescence-based sensing materials as an approach for the selective detection of a specific analyte. Furthermore, the rheological properties exhibited by gel **1-Zn²⁺** were similar to those of a typical hydrogel. The present results emphasize the validity of ligand design that includes metal-binding in realizing metal–organic framework gel systems with versatile and stimuli-responsive properties. These concepts should bring about the development of a wide range of responsive soft materials.

Experimental Section

General considerations: 2,4-dinitrotoluene (DNT) was purchased from TCI and re-crystallized from ethanol. 2,4,6-Trinitrotoluene (TNT) was prepared from DNT using literature procedures.^[45] All other chemicals were purchased from Aldrich, TCI, or Wako and used as received. ¹H and ¹³C NMR spectra were measured on a Bruker ARX 300 apparatus. IR spectra were obtained for KBr pellets, in the range 400–4000 cm⁻¹, with a Shimadzu FT-IR 8400S, and mass spectra were obtained by a JEOL JMS-700 mass spectrometer. The optical absorption spectra of the samples were obtained at 298 K using a UV/Vis spectrophotometer (Hitachi U-2900). All fluorescence spectra were recorded in RF-5301PC spectrophotometer. The accelerating voltage of SEM was 5–15 kV and the emission current was 10 μA.

Fluorescence lifetime microscopy (FLM) measurements: Fluorescence lifetime images were acquired by an inverse time resolved fluorescence microscope, MicroTime-200 (PicoQuant GmbH). The excitation wavelength, the spatial resolution, and the time resolution were 405 nm, 0.3 μm, and 60–70 ps, respectively. The samples were prepared on one side of microscope cover glasses. The manufacturer's software was used to analyze the data and calculate the lifetime maps. The color scales represent average lifetime and total number of counts is indicated by color density at each point.

Fluorescence confocal microscopy: Images were recorded on Nikon Microscope ECLIPSE 80i using UV light (400 nm) as the excitation source, and the emission was collected between 340–480 nm with 100× magnification. Samples were prepared by drop-casting on a glass slide followed by slow evaporation.

Rheological measurements: These were carried out on freshly prepared gels by using a controlled stress rheometer (AR-1000N, TA Instruments Ltd., New Castle, DE, USA). A parallel plate geometry of 40 mm diameter and 1.5 mm gap was employed throughout. Following loading, the exposed edges of samples were covered with a silicone fluid from BDH (100 centistokes (cs)) to prevent water loss. Dynamic oscillatory work kept a frequency of 1.0 rad s⁻¹. The following tests were performed: increasing amplitude of oscillation up to 100% apparent strain on shear, time, and frequency sweeps at 25 °C (60 min and from 0.1–100 rad s⁻¹, respectively). Unidirectional shear routines were performed at 25 °C covering a shear-rate regime between 10⁻¹ and 10³ s⁻¹. Mechanical spectroscopy routines were completed with transient measurements. In doing so, the desired stress was applied instantaneously to the sample and the angular displacement was monitored for 60 min (retardation curve). After

completion of the run, the imposed stress was withdrawn and the extent of structure recovery was recorded for another 60 min (relaxation curve). Dynamic and steady shear measurements were conducted in triplicate and creep (transient) measurements in duplicate. The rheological properties of gel **1** (2.0 wt%) with Zn²⁺ (3.0 equiv) were measured at 25.0 °C.

X-ray powder diffraction: The X-ray powder diffraction (XRPD) experiments were performed in a transmission mode with a Bruker GADDS diffractometer equipped with graphite monochromated Cu_{Kα} radiation (λ = 1.54073 Å). The samples were prepared by freeze-drying the hydrogel **1-Zn²⁺** (2.0 wt%).

SEM Observation: Scanning electron micrographs of the samples were taken with a field emission scanning electron microscope (FE-SEM, Philips XL30 S FEG). The accelerating voltage of SEM was 5–15 kV and the emission current was 10 μA.

Preparation of hydrogel **1-Zn²⁺:** In a vial, ligand **1** (5 mg) was added to 0.1 M NaOH solution (200 μl) of in the presence of Zn²⁺ (2.0 equiv). The hydrogel was formed immediately after ultrasonication in ambient temperature.

Preparation of filter paper test strips: Filter paper (10×2 cm) test strips were prepared by coating with the melted hydrogel **1-Zn²⁺** (2.0 wt%) followed by removal of solvent under vacuum at room temperature. The gel-coated filter papers were then cut into 10 pieces (0.5×0.5 cm) to obtain the test strips, which were then used for the detection of explosives.

Detection of explosive analytes by emission quenching: The required analyte solutions of various concentrations (1×10⁻¹²–1×10⁻³ M) were added to each strip, and the solvents were allowed to evaporate. The film was placed in such a way that the excitation beam falls on the spot where explosive analyte is added. Emission was collected by a front-face technique by using a film sample holder. Emission of a blank sample was monitored by the addition of solvent alone.

Compound 2: Methyl 4-(chlorocarbonyl)benzoate **4** (0.5 g, 2.5 mmol) in THF was added to 2,6-diaminopyridine **3** (1.02 g, 1.25 mmol) and a solution of pyridine (0.148 mL, 1.25 mmol). The reaction mixture was stirred at 25 °C for 2 h and then was removed solvent by evaporation. The crude product was purified by column chromatography on silica gel with dichloromethane (R_f=0.5). Yield 63%. ¹H NMR (300 MHz, [D₆]DMSO): δ = 10.7 (s, 2H, NH), 8.2 (m, 8H, Ar-H), 7.9 (m, 3H, Ar-H), 3.9 ppm (s, 6H, -CH₃); ¹³C NMR ([D₆]DMSO): δ = 166, 165, 160, 139, 138, 135, 133, 128, 99, 51 ppm; IR (KBr): ν̄ = 3337, 3009, 2950, 1708, 1639, 1590, 1511, 1442, 1314, 1274, 1096, 1008, 899, 870, 790, 731, 632 cm⁻¹; HRMS (FAB⁺): *m/z* calcd for C₂₃H₁₉N₃O₆: 434.3562 [M+H⁺]; found: 434.4135; elemental analysis calcd (%) for C₂₃H₁₉N₃O₆: C 63.74, H 4.42, N 9.70, O 22.15; found: C 63.92, H 4.23, N 9.68.

Compound 1: Compound **2** (0.3 g, 0.7 mmol) in THF (10 mL) was added to a solution of NaOH (0.7 g, 3.5 mmol). The reaction mixture was heated at reflux for 3–4 h at 70 °C and then cooled to room temperature. Then, an aqueous solution of HCl (1.0 M) was slowly added to the reaction mixture (pH 3–4). The product was obtained as a white powder. Yield 40%. ¹H NMR (300 MHz, [D₆]DMSO): δ = 13.25 (s, 2H, OH), 10.74 (s, 2H, NH), 8.2 (m, 8H, Ar-H), 7.9 (m, 3H, Ar-H); ¹³C NMR ([D₆]DMSO): δ = 169, 165, 158, 139, 134, 130, 128, 127, 99 ppm; IR (KBr): ν̄ = 3419, 1705 m 1542, 1421, 1232, 1110, 665 cm⁻¹; HRMS (FAB⁺): *m/z* calcd (%) for C₂₁H₁₅N₃O₆: 406.2968 [M+H⁺]; found: 406.3603; analysis calcd (%) for C₂₁H₁₅N₃O₆: C 62.22, H 3.73, N 10.37, O 23.68. found: C 62.48, H 3.72, N 10.42.

Acknowledgements

This work was supported by a grant from the Program (R32-2008-000-20003-0) and the NRF (2012002547) supported from the Ministry of Education, Science and Technology, Korea. In addition, this work was partially supported by a grant from the Next-Generation BioGreen 21 Program (SSAC, grant No.: PJ009041022012), Rural development Administration, Korea.

- [1] A. Fainberg, *Science* **1992**, 255, 1531.
- [2] K. J. Albert, N. S. Lewis, C. L. Schauer, G. A. Sotzing, S. E. Stitzel, T. P. Vaid, D. R. Walt, *Chem. Rev.* **2000**, 100, 2595.
- [3] T. H. Kim, B. Y. Lee, J. Jaworski, K. Yokoyama, W.-J. Chung, E. Wang, S. Hong, A. Majumdar, S.-W. Lee, *ACS Nano* **2011**, 5, 2824.
- [4] A. L. Pinnaduwaage, A. Gehl, D. L. Hedden, G. Muralidharan, T. Thundat, R. T. Lareau, T. Sulchek, L. Manning, B. Rogers, M. Jones, J. D. Adams, *Nature* **2003**, 425, 474.
- [5] W. E. Tenhaeff, L. D. McIntosh, K. K. Gleason, *Adv. Funct. Mater.* **2010**, 20, 1144.
- [6] A. W. Czarnik, *Nature* **1998**, 394, 417.
- [7] M. E. Germain, M. J. Knapp, *Chem. Soc. Rev.* **2009**, 38, 2543.
- [8] Y. Salinas, R. Martinez-Manez, M. D. Marcos, F. Sancenon, A. M. Costero, M. Parra, S. Gil, *Chem. Soc. Rev.* **2012**, 41, 1261.
- [9] E. R. Goldman, I. L. Medintz, J. L. Whitley, A. Hayhurst, A. R. Clapp, H. T. Uyeda, J. R. Deschamps, M. E. Lassman, H. Mattoussi, *J. Am. Chem. Soc.* **2005**, 127, 6744.
- [10] A. Lan, K. Li, H. Wu, D. H. Olson, T. J. Emge, W. Ki, M. Hong, J. Li, *Angew. Chem.* **2009**, 121, 2370; *Angew. Chem. Int. Ed.* **2009**, 48, 2334.
- [11] S. Pramanik, C. Zheng, X. Zhang, T. J. Emge, J. Li, *J. Am. Chem. Soc.* **2011**, 133, 4153.
- [12] M. B. Pushkarsky, I. G. Dunayevskiy, M. Prasanna, A. G. Tsekoun, R. Go, C. K. N. Patel, *Proc. Natl. Acad. Sci. USA* **2006**, 103, 19630.
- [13] J.-S. Yang, T. M. Swager, *J. Am. Chem. Soc.* **1998**, 120, 11864.
- [14] J.-S. Yang, T. M. Swager, *J. Am. Chem. Soc.* **1998**, 120, 5321.
- [15] D. T. McQuade, A. E. Pullen, T. M. Swager, *Chem. Rev.* **2000**, 100, 2537.
- [16] S. Zahn, T. M. Swager, *Angew. Chem.* **2002**, 114, 4399; *Angew. Chem. Int. Ed.* **2002**, 41, 4225.
- [17] A. Rose, Z. Zhu, C. F. Madigan, T. M. Swager, V. Bulovi, *Nature* **2005**, 434, 876.
- [18] S. W. Thomas, G. D. Joly, T. M. Swager, *Chem. Rev.* **2007**, 107, 1339.
- [19] T. M. Swager, *Acc. Chem. Res.* **2008**, 41, 1181.
- [20] H. Sohn, R. M. Calhoun, M. J. Sailor, W. C. Trogler, *Angew. Chem.* **2001**, 113, 2162; *Angew. Chem. Int. Ed.* **2001**, 40, 2104.
- [21] H. Sohn, M. J. Sailor, D. Magde, W. C. Trogler, *J. Am. Chem. Soc.* **2003**, 125, 3821.
- [22] S. J. Toal, D. Magde, W. C. Trogler, *Chem. Commun.* **2005**, 5465.
- [23] J. C. Sanchez, A. G. DiPasquale, A. L. Rheingold, W. C. Trogler, *Chem. Mater.* **2007**, 19, 6459.
- [24] J. C. Sanchez, W. C. Trogler, *J. Mater. Chem.* **2008**, 18, 3143.
- [25] K. Zhang, H. Zhou, Q. Mei, S. Wang, G. Guan, R. Liu, J. Zhang, Z. Zhang, *J. Am. Chem. Soc.* **2011**, 133, 8424.
- [26] M. Riskin, R. Tel-Vered, I. Willner, *Adv. Mater.* **2010**, 22, 1387.
- [27] W. G. Qu, B. Deng, S. L. Zhong, H. Y. Shi, S. S. Wang, A. W. Xu, *Chem. Commun.* **2011**, 47, 1237.
- [28] M. Riskin, R. T. Vered, T. Bourenko, E. Granot, I. Willner, *J. Am. Chem. Soc.* **2008**, 130, 9726.
- [29] M. Riskin, R. Tel-Vered, O. Lioubashevski, I. Willner, *J. Am. Chem. Soc.* **2009**, 131, 7368.
- [30] K. K. Kartha, S. S. Babu, S. Srinivasan, A. Ajayaghosh, *J. Am. Chem. Soc.* **2012**, 134, 4834.
- [31] A. Ajayaghosh, V. K. Praveen, *Acc. Chem. Res.* **2007**, 40, 644.
- [32] A. Ajayaghosh, V. K. Praveen, C. Vijayakumar, *Chem. Soc. Rev.* **2008**, 37, 109.
- [33] T. Cardolaccia, Y. Li, K. S. Schanze, *J. Am. Chem. Soc.* **2008**, 130, 2535.
- [34] S. S. Babu, K. K. Kartha, A. Ajayaghosh, *J. Phys. Chem. Lett.* **2010**, 1, 3413.
- [35] H. Kim, T. Kim, M. Lee, *Acc. Chem. Res.* **2011**, 44, 72.
- [36] A. Ajayaghosh, V. K. Praveen, C. Vijayakumar, S. J. George, *Angew. Chem.* **2007**, 119, 6376; *Angew. Chem. Int. Ed.* **2007**, 46, 6260.
- [37] C. Vijayakumar, V. K. Praveen, A. Ajayaghosh, *Adv. Mater.* **2009**, 21, 2059.
- [38] L. Zang, Y. Che, J. S. Moore, *Acc. Chem. Res.* **2008**, 41, 1596.
- [39] G. V. Zyryanov, M. A. Palacios, P. Anzenbacher, *Org. Lett.* **2008**, 10, 3681.
- [40] C. Vijayakumar, G. Tobin, W. Schmitt, M. J. Kima, M. Takeuchi, *Chem. Commun.* **2010**, 46, 874.
- [41] B. An, S. Kwon, S. Jung, S. Y. Park, *J. Am. Chem. Soc.* **2002**, 124, 14410.
- [42] H. Lee, S. H. Jung, W. S. Han, J. H. Moon, S. Kang, J. Y. Lee, J. H. Jung, S. Shinkai, *Chem. Eur. J.* **2011**, 17, 2823.
- [43] K. K. Kartha, R. D. Mukhopadhyay, A. Ajayaghosh, *Chimia* **2013**, 67, 51.
- [44] S. Barman, J. A. Garg, O. Blacque, K. Venkatesan, H. Berke, *Chem. Commun.* **2012**, 48, 11127.
- [45] F. D. Lewis, J. S. Yang, C. L. Stern, *J. Am. Chem. Soc.* **1996**, 118, 12029.
- [46] Gaussian 03, Revision B.05, M. J. Frisch, G. W. Trucks, H. B. Schlegel, G. E. Scuseria, M. A. Robb, J. R. Cheeseman, J. A. Montgomery, Jr., T. Vreven, K. N. Kudin, J. C. Burant, J. M. Millam, S. S. Iyengar, J. Tomasi, V. Barone, B. Mennucci, M. Cossi, G. Scalmani, N. Rega, G. A. Petersson, H. Nakatsuji, M. Hada, M. Ehara, K. Toyota, R. Fukuda, J. Hasegawa, M. Ishida, T. Nakajima, Y. Honda, O. Kitao, H. Nakai, M. Klene, X. Li, J. E. Knox, H. P. Hratchian, J. B. Cross, V. Bakken, C. Adamo, J. Jaramillo, R. Gomperts, R. E. Stratmann, O. Yazyev, A. J. Austin, R. Cammi, C. Pomelli, J. W. Ochterski, P. Y. Ayala, K. Morokuma, G. A. Voth, P. Salvador, J. J. Dannenberg, V. G. Zakrzewski, S. Dapprich, A. D. Daniels, M. C. Strain, O. Farkas, D. K. Malick, A. D. Rabuck, K. Raghavachari, J. B. Foresman, J. V. Ortiz, Q. Cui, A. G. Baboul, S. Clifford, J. Cioslowski, B. B. Stefanov, G. Liu, A. Liashenko, P. Piskorz, I. Komaromi, R. L. Martin, D. J. Fox, T. Keith, M. A. Al-Laham, C. Y. Peng, A. Nanayakkara, M. Challacombe, P. M. W. Gill, B. Johnson, W. Chen, M. W. Wong, C. Gonzalez, J. A. Pople, Gaussian, Inc., Wallingford CT, **2004**.
- [47] D. R. Shankaran, K. V. Gobi, T. Sakai, K. Matsumoto, K. Toko, N. Miura, *Biosens. Bioelectron.* **2005**, 20, 1750.
- [48] H.-X. Zhang, A.-M. Cao, J.-S. Hu, L.-J. Wan, S.-T. Lee, *Anal. Chem.* **2006**, 78, 1967.
- [49] J. Wang, S. B. Hocevar, B. Ogorevc, *Electrochem. Commun.* **2004**, 6, 176.
- [50] Strategic Diagnostics, Inc., Analysis of TNT and RDX in Groundwater, <http://www.sdx.com>.
- [51] S. Hrapovic, E. Majid, Y. Liu, K. Male, J. H. T. Luong, *Anal. Chem.* **2006**, 78, 5504.
- [52] H.-X. Zhang, J.-S. Hu, C.-J. Yan, L. Jiang, L.-J. Wan, *Phys. Chem. Chem. Phys.* **2006**, 8, 3567.
- [53] Larsson, J. Angbrant, J. Ekeröth, P. Mansson, B. Liedberg, *Sens. Actuators B* **2006**, 113, 730.
- [54] L. C. Shriver-Lake, K. A. Breslin, P. T. Charles, D. W. Conrad, J. P. Golden, F. S. Ligler, *Anal. Chem.* **1995**, 67, 2431.
- [55] J. Wang, R. K. Bhada, J. Lu, D. MacDonald, *Anal. Chim. Acta* **1998**, 361, 85.

Received: April 20, 2013

Revised: September 9, 2013

Published online: November 6, 2013